

A histomorphometric comparison of the muscular tissue reaction to stainless steel, pure titanium and titanium alloy implant materials

M. THERIN, A. MEUNIER, P. CHRISTEL

Laboratoire de Recherches Orthopédiques, 10 Avenue de Verdun, F 75010 Paris, France

The *in vivo* tissue reaction to titanium and titanium-based alloys using quantitative histomorphometry was investigated. According to the guidelines for biomaterials testing suggested by ISO, 2 mm × 6 mm cylindrical specimens of chemically pure (CP) Ti, TiO₂, electrolytically coated Ti, Ti6Al4V, TiO₂-coated Ti6Al4V, TiN physical vapour deposition-coated Ti6Al4V and Ti5Al2.5Fe were implanted in the paravertebral muscles of rats, for 1–52 weeks, 316L stainless steel being used as a control implant material. After PMMA embedding, electrochemical dissolution of the implants, microtome sectioning and Masson's trichrome staining, the tissue reaction was assayed using a semi-automatic method based on the digitization of both the encapsulating membrane contours and the different cell types located within it. All materials induced a close tissue reaction. There was no statistical difference between the tested materials regarding the time-evolution of the inflammatory cells. However, when comparing CP Ti with 316L, a significant difference was found in the fibrocyte kinetics: in the short term, fibrocyte densities were lower for 316L, while beyond 12 weeks, they exhibited higher values than CP Ti. To a lesser extent, a similar observation was made when comparing CP Ti with Ti5Al2.5Fe. No statistical difference was found in the comparison of CP Ti with Ti6Al4V. The membrane thickness was identical for all tested materials and appeared not to be time-dependent.

1. Introduction

For over twenty years, titanium and particularly its aluminium–vanadium alloy, have been extensively used in dentistry, implantology and orthopaedic surgery. Owing to a higher corrosion resistance, as well enhanced fatigue strength, these alloys have been considered as an interesting alternative to previously used stainless steel and cobalt–chromium alloys. However, in the long term, the presence of vanadium in this alloy may be a cause for concern. Although vanadium in Ti6Al4V alloy is very stable and the amount of ion-release found in the normal situation is always lower than the toxic level [1], intrinsic vanadium toxicity is well known and can be potentiated when an implant is fractured or submitted to fretting [2].

In order to avoid this potential risk, several solutions have been proposed: either cover the alloy with a TiO₂ or TiN layer to minimize ion release, or use vanadium-free alloys (Ti5Al2.5Fe and Ti6Al7Nb, for example).

The literature survey shows that the assay of the biological properties of these materials using quantitative histomorphometry is fragmentary. Thus, the purpose of this study was to compare the tissue reaction to pure titanium (CP Ti) and some of its alloys by using a quantitative histomorphometric method in order to rank these materials according to

their composition or surface treatment [6–10]. The statistical analysis of the distribution parameters of the different cell types involved in the tissue response, arising from histomorphometry, permits a quantitative comparison of the materials [11].

2. Materials and methods

2.1. Implants

Cylinders (2 mm o.d. and 6 mm long) having a surface roughness as good as possible for such small implants (0.1–0.2 μm Ra) were used. Scanning electron micrographs of the implants are shown in Fig. 1. In this experiment, four materials were compared: 316L, CP Ti, Ti6Al4V, Ti5Al2.5Fe.

Two different coating procedures were also tested: one on CP Ti (TiO₂ coating) and two on Ti6Al4V (TiO₂ and TiN coatings). The TiO₂ coating (thickness 0.2 μm) was obtained by electrolytical anodization and the TiN coating (thickness 1 μm) by physical vapour deposition (PVD). The characteristics of the implant materials are listed in Table I. The implants were ultrasonically cleaned, individually packed in double-sterile packaging (Sterilsop Soplamed), and sterilized in an autoclave at 133°C. CP Ti was used as the control material.

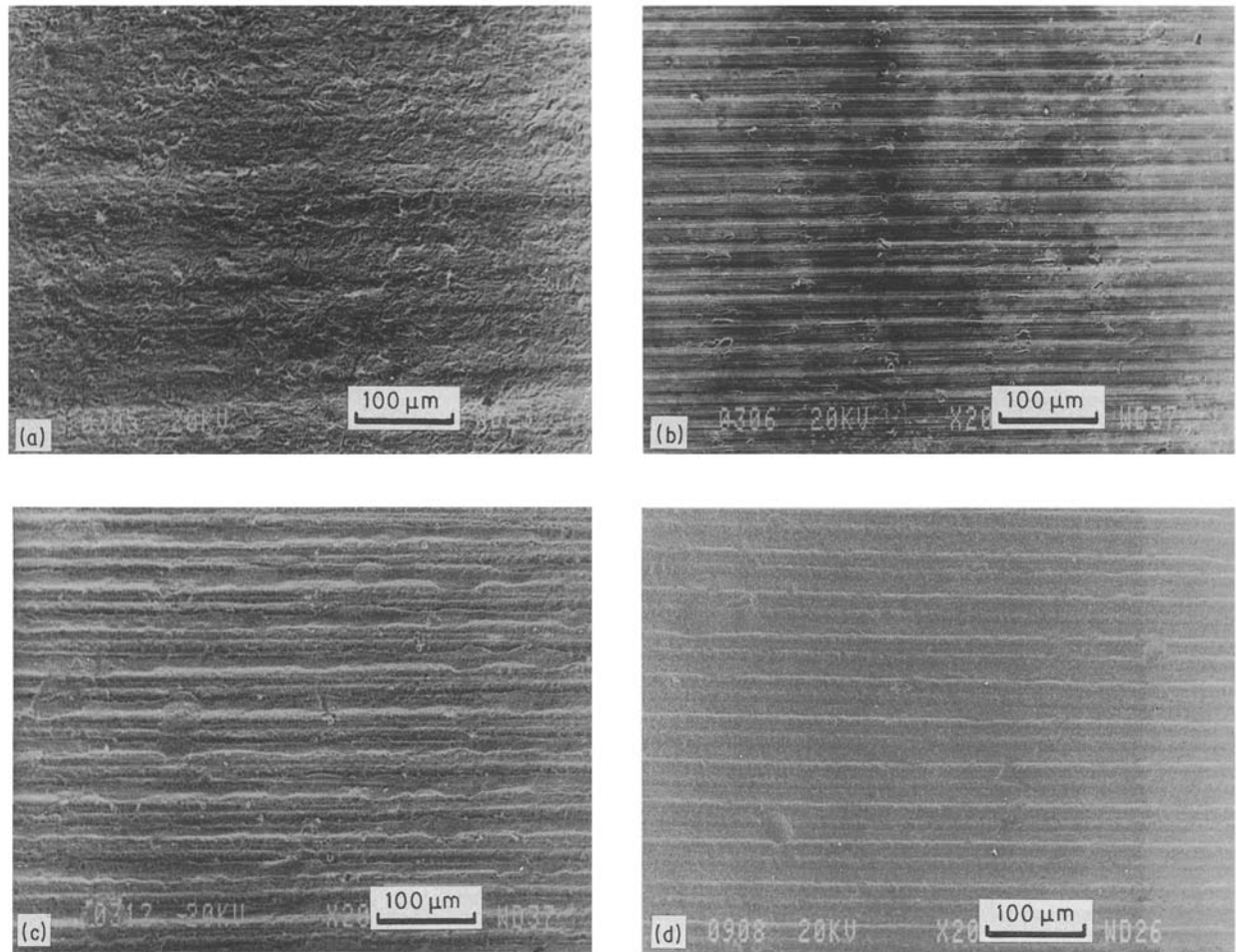


Figure 1 Scanning electron micrographs showing a close surface appearance of the implants used in this study. (a) Ti, (b) 316L, (c) Ti6Al4V, (d) TiO₂-coated Ti6Al4V.

TABLE I Characteristics of the materials used in the current study

Material	Source	Standard	Manufacturing proc.	Roughness ($\mu\text{m Ra}$)
CP Ti	Cezus (Pechiney)	ISO 5832/11	cast	0.1–0.2
316L SS	Ugine	NF S 90-401	wrought	0.1–0.2
Ti6Al4V	Cezus (Pechiney)	ISO 5832/3	wrought	0.1–0.2
Ti5Al2.5Fe	Krupp	—	wrought	0.1–0.2
Ti–TiO ₂	Cezus (Pechiney)	ISO 5832/11	cast + anodiz.	0.1–0.2
Ti6Al4V–TiO ₂	Cezus (Pechiney)	ISO 5832/3	wrought + anodiz.	0.1–0.2
Ti6Al4V–TiN	Cezus (Pechiney)	ISO 5832/3	wrought + PVD	0.1–0.2

2.2. Animals and surgical procedure

Non-inbred Sprague-Dawley rats, weighing 250–350 g at surgery, were used. The surgery was performed under general anaesthesia in semisterile conditions. The fur was clipped and the skin scrubbed with polyvidone iodine solution. A 1 cm skin incision was made on the spinous process line. No direct surgical approach was performed in order to limit the influence of the non-specific surgical trauma. One sterile implant was pushed through a 2.4 mm i.d. trocar driven from the incision into the paravertebral muscles of the lumbar area, on each side of the spine, each animal receiving two different implant materials. The skin incision was closed with stainless steel staples.

The animals were sacrificed after 1, 2, 4, 12, 26 and 52 weeks post-implantation. The number of implants

finally available per material for each group sacrificed is listed in Table II.

2.3. Implant and tissue processing

The procedure was conducted according to a method previously described [12]. After sacrifice, the implant and surrounding muscles were removed *en bloc*, fixed in formalin, dehydrated in ethanol and embedded in polymethylmethacrylate. Electrodissection was used in order to remove delicately the metallic part of the implant while keeping intact the actual tissue–implant interface. Sections 5 μm long were cut on a Polycut microtome, perpendicular to the implant axis, at 2 mm from the tip of the implant, to avoid the influence of the sharp edges on the tissue reaction. Histological

TABLE II Number of specimens available for the histomorphometric analysis per material, and time of observation

Material	No. of specimens					
	1 week	2 weeks	4 weeks	12 weeks	26 weeks	52 weeks
Ti	8	7	8	6	7	3
316L	7	6	7	4	4	0
Ti6Al4V	4	5	7	6	7	2
Ti5Al2.5Fe	5	4	6	5	6	5
Ti-TiO ₂	3	6	8	7	6	3
Ti6Al4V-TiO ₂	5	5	6	7	9	2
Ti6Al4V-TiN	4	6	8	6	3	6

sections were routinely stained with Masson's trichrome (Fig. 2).

2.4. Computer-assisted-cell-counting

The sections were observed at a $\times 400$ magnification with an Olympus BHT microscope, equipped with a drawing tube. The image of the histological section was digitized via the diode-cursor of a graphic-tablet, driven by an IBM-AT compatible micro-computer. For each optical field, the observer digitized the membrane contours and then, separately, the nuclei of the following cells: fibrocytes, macrophages, polymorphonuclear cells (PMN), round mononuclear cells (lymphocytes, plasma cells, mast cells), multinucleated giant cells, and unidentified cells. The procedure was repeated routinely at least on seven separate optical fields of the membrane. For each digitized section, the maximum, minimum, and average membrane thickness, as well as the distribution parameters of each cell type, (when in sufficient numbers), were computed with an in-house software (DIGICELL). Means and standard deviations for each parameter were calculated to allow a statistical analysis.

The parameters thus computed were divided into four groups:

1. a group of distance parameters including membrane thickness and various location of quantile for different cell types;
2. a group of linear densities taking into account the number of cells found per millimetre of digitized membrane;
3. a group of surface densities including cell densities at various quantiles;
4. finally, a group of parameters describing the theoretical cell distribution. It has been shown previously [12] that the cell maximum is not located at the material-tissue interface and the cells are not randomly distributed. Among various possible theoretical distributions, the Weibull model has been found to exhibit the best fit with the observed cell distribution [13, 14].

This model can be described by three parameters, μ , λ and σ . λ is a shape parameter which represents the asymmetry of the curve, σ is a scale parameter and μ corresponds to a location parameter which relates to the distance between the origin of the cell distribution and the material-tissue interface. In all cases of the

current study, μ was found to be smaller than $3 \mu\text{m}$ and subsequently considered equal to $0 \mu\text{m}$. The statistical analysis was performed by using the Student *t*-test.

3. Results

The first observation which was a common character to all materials, was the very specific non-Gaussian pattern exhibited by the cell distribution. The cell distribution in the encapsulated membrane from the implant-tissue interface to the normal muscular tissue exhibited an asymmetric bell-shape curve (Fig. 3), already described [11, 12] for other biomaterials. The number of cells increased from the interface to rapidly reach the maximum and then decreased at a much lower rate. The maximum location of macrophages was closer to the implant-tissue interface when compared to the fibrocytes. While the fibrocytes covered almost the entire membrane surface, the macrophages appeared located only in an area close to the interface. The density of the cells decreased with time, and at 52 weeks, only less than 50% of the initial amount was still present (Fig. 4). The percentage of unidentified cells is not time dependent and always around 5%.

In order to compare all the materials for all the implantation times, the different histomorphometric parameters previously described were used. For the materials investigated in this study, there was no

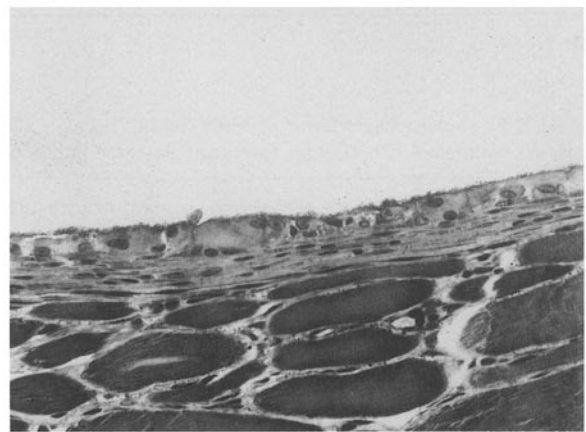


Figure 2 Photomicrograph of a typical area surrounding a TiN-coated Ti6Al4V implant taken at the magnification used for the cell counting procedure (Masson's Trichrome, $\times 240$).

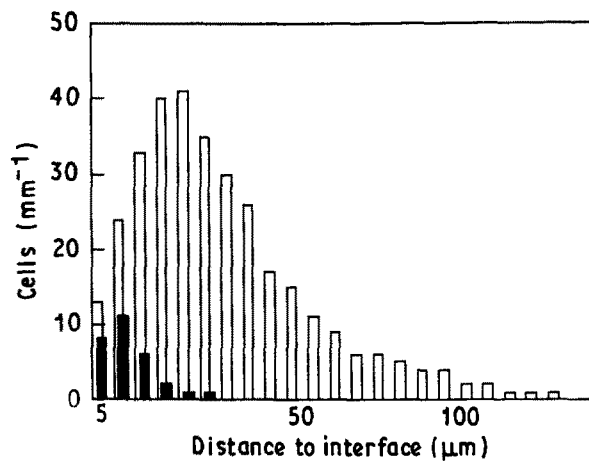


Figure 3 Cell distribution for (□) fibrocytes and (■) macrophages in the membrane encapsulating a CP Ti specimen, 1 week after implantation. Each class interval corresponds to a 5 μm membrane layer. The cell distribution follows a non-Gaussian pattern the best fit of which can be modelled by the Weibull model.

statistical significant difference in the membrane thickness when comparing all materials for all implantation times. The membrane thickness was not a time-dependent parameter (Fig. 5); its value was always in the 40–60 μm range for all materials with no significant difference. Accordingly, the membrane thickness was not taken into account to assay differences in the local biocompatibility.

Regardless of the implant material, PMNs were found at low concentrations and were not noted beyond 2 weeks post-implantation. The most representative data of the calculated parameters for the other cell types are listed in Tables III–VIII.

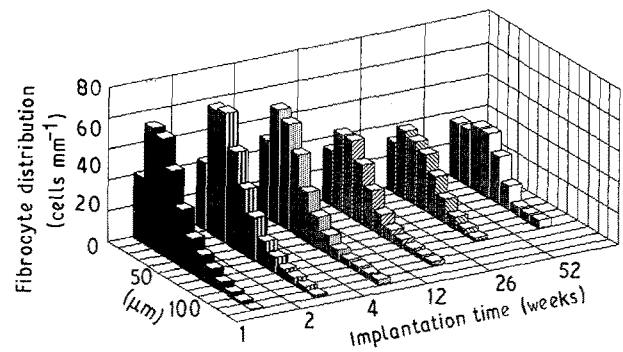


Figure 4 Overall time evolution of fibrocyte distributions in the encapsulating membrane (10 μm class intervals). Fibrocyte numbers decrease in amplitude and distance from the tissue–implant interface with time.

3.1. CP Ti–Ti6Al4V comparison

In this experiment, no differences were observed between the twenty computed parameters, at any time of implantation. CP Ti and Ti6Al4V induced an identical tissue reaction in the rat muscles.

3.2. CP Ti–316L comparison (Fig. 6)

The statistical analysis exhibited the following data:

linear density of fibrocytes:

- $p < 0.02$ at 1 week (Ti > 316L)
- $p = 0.07$ at 2 weeks (Ti > 316L)
- $p < 0.05$ at 26 weeks (Ti < 316L)

TABLE III Fibrocyte linear densities (mean ± s.d.) at each period of observation for all implanted materials

Material	Fibrocyte linear density (cells mm ⁻¹)					
	1 week	2 weeks	4 weeks	12 weeks	26 weeks	52 weeks
Ti	330 ± 50	354 ± 91	229 ± 69	213 ± 56	156 ± 50	81 ± 8
316L	260 ± 89	237 ± 90	217 ± 46	180 ± 27	230 ± 59	■
Ti6Al4V	344 ± 173	306 ± 136	266 ± 88	155 ± 28	163 ± 44	■
Ti5Al2.5Fe	285 ± 51	351 ± 130	332 ± 142	178 ± 34	142 ± 41	184 ± 57
Ti–TiO ₂	182 ± 35	279 ± 94	254 ± 110	174 ± 60	198 ± 44	144 ± 12
Ti6Al4V–TiO ₂	257 ± 63	320 ± 109	226 ± 101	193 ± 78	126 ± 24	■
Ti6Al4V–TiN	293 ± 90	311 ± 79	295 ± 65	186 ± 82	124 ± 24	169 ± 38

(■) Not available

TABLE IV Macrophages linear densities (mean ± s.d.) for all implanted materials. When data are in insufficient number for statistical analysis, minimum and maximum values are presented in parentheses

Material	Macrophage linear density (cells mm ⁻¹)					
	1 week	2 weeks	4 weeks	12 weeks	26 weeks	52 weeks
Ti	28 ± 35	39 (0–176)	3 (0–20)	5 (0–28)	0	0
316L	54 ± 46	35 (0–53)	0	0	0	■
Ti6Al4V	68 ± 52	10 (0–31)	1 (0–10)	0	0	■
Ti5Al2.5Fe	12 ± 20	16 (0–39)	12 (0–49)	2 (0–12)	1 (0–5)	0
Ti–TiO ₂	17 ± 29	24 (0–73)	3 (0–16)	0	0	0
Ti6Al4V–TiO ₂	27 ± 10	20 (0–65)	12 (0–27)	5 (0–20)	0	■
Ti6Al4V–TiN	22 ± 11	25 (3–71)	6 (0–22)	0	0	0

(■) Not available

TABLE V Median distance of fibrocytes from interface (mean \pm S.D.) for all implanted materials at each time of observation

Material	Median distance from interface (μm)					
	1 week	2 weeks	4 weeks	12 weeks	26 weeks	52 weeks
Ti	26 \pm 7	28 \pm 13	22 \pm 6	35 \pm 6	28 \pm 12	26 \pm 9
316L	33 \pm 12	25 \pm 8	23 \pm 7	24 \pm 10	26 \pm 9	■
Ti6Al4V	34 \pm 12	27 \pm 7	23 \pm 5	27 \pm 10	33 \pm 6	■
Ti5Al2.5Fe	20 \pm 5	25 \pm 6	30 \pm 12	26 \pm 15	32 \pm 11	21 \pm 5
Ti-TiO ₂	18 \pm 8	26 \pm 8	30 \pm 10	23 \pm 5	28 \pm 7	26 \pm 6
Ti6Al4V-TiO ₂	21 \pm 6	26 \pm 14	19 \pm 6	28 \pm 8	23 \pm 6	■
Ti6Al4V-TiN	32 \pm 13	30 \pm 8	26 \pm 3	30 \pm 14	19 \pm 5	29 \pm 9

(■) Not available

TABLE VI Membrane surface densities of fibrocytes (mean \pm S.D.) for all implanted materials at each time of observation

Material	Fibrocyte membrane surface density (10^3 cells mm^{-2})					
	1 week	2 weeks	4 weeks	12 weeks	26 weeks	52 weeks
Ti	6.29 \pm 1.35	6.38 \pm 1.08	5.26 \pm 0.94	3.24 \pm 0.46	3.42 \pm 0.89	1.75 \pm 0.36
316L	3.90 \pm 0.96	4.61 \pm 0.88	4.94 \pm 1.15	4.64 \pm 1.94	5.28 \pm 2.07	■
Ti6Al4V	5.93 \pm 2.30	5.48 \pm 1.61	5.55 \pm 1.60	3.75 \pm 1.15	2.93 \pm 0.83	■
Ti5Al2.5Fe	6.61 \pm 0.42	6.36 \pm 2.28	5.73 \pm 2.46	4.02 \pm 1.50	2.56 \pm 0.67	4.58 \pm 1.56
Ti-TiO ₂	4.98 \pm 1.83	5.90 \pm 1.36	4.03 \pm 0.96	3.89 \pm 1.31	3.74 \pm 0.77	3.10 \pm 1.13
Ti6Al4V-TiO ₂	5.70 \pm 1.22	5.93 \pm 1.53	5.01 \pm 1.93	3.55 \pm 1.63	2.82 \pm 0.51	■
Ti6Al4V-TiN	4.14 \pm 1.88	5.05 \pm 1.55	5.29 \pm 0.75	3.50 \pm 1.25	3.05 \pm 0.67	3.56 \pm 0.86

TABLE VII λ , theoretical parameter (see text) for fibrocyte distribution, for all materials at each time of observation

Material	λ					
	1 week	2 weeks	4 weeks	12 weeks	26 weeks	52 weeks
Ti	1.67 \pm 0.35	1.92 \pm 0.63	1.77 \pm 0.19	1.74 \pm 0.50	2.02 \pm 0.51	1.90 \pm 0.25
316L	1.64 \pm 0.39	1.93 \pm 0.50	1.73 \pm 0.31	1.83 \pm 0.14	1.76 \pm 0.13	■
Ti6Al4V	2.09 \pm 0.15	1.98 \pm 0.18	1.78 \pm 0.34	2.03 \pm 0.24	1.76 \pm 0.23	■
Ti5Al2.5Fe	1.96 \pm 0.27	1.73 \pm 0.16	1.73 \pm 0.25	1.82 \pm 0.34	1.93 \pm 0.34	1.73 \pm 0.14
Ti-TiO ₂	1.79 \pm 0.34	1.90 \pm 0.40	1.67 \pm 0.26	1.89 \pm 0.31	1.81 \pm 0.20	1.62 \pm 0.20
Ti6Al4V-TiO ₂	1.72 \pm 0.18	1.54 \pm 0.29	1.53 \pm 0.37	1.76 \pm 0.27	1.71 \pm 0.34	■
Ti6Al4V-TiN	1.82 \pm 0.40	1.76 \pm 0.37	1.69 \pm 0.12	1.94 \pm 0.27	1.69 \pm 0.26	1.89 \pm 0.49

(■) Not available

TABLE VIII σ , theoretical parameter (see text) for fibrocyte distribution, for all materials at each time of observation

Material	σ					
	1 week	2 weeks	4 weeks	12 weeks	26 weeks	52 weeks
Ti	34.4 \pm 9.1	36.6 \pm 13.6	25.7 \pm 6.4	41.2 \pm 5.8	30.6 \pm 12.5	28.9 \pm 7.6
316L	41 \pm 13.3	30.5 \pm 9.0	26.5 \pm 7.1	25.2 \pm 11.0	27.8 \pm 7.6	■
Ti6Al4V	40.2 \pm 14.1	32.4 \pm 8.2	29.0 \pm 6.9	30.2 \pm 10.1	35.1 \pm 5.6	■
Ti5Al2.5Fe	24.9 \pm 3.7	31.2 \pm 4.8	35.7 \pm 14.9	29.5 \pm 15.6	36.4 \pm 9.9	24.5 \pm 4.0
Ti-TiO ₂	21.2 \pm 7.9	31.5 \pm 9.9	37.8 \pm 15.7	27.3 \pm 5.2	32.7 \pm 7.9	30.1 \pm 11.2
Ti6Al4V-TiO ₂	26.8 \pm 8.0	33.2 \pm 14.5	26.4 \pm 5.1	33.9 \pm 5.8	27.4 \pm 5.8	■
Ti6Al4V-TiN	37.8 \pm 18.2	37.7 \pm 14.2	32.5 \pm 4.6	33.9 \pm 13.9	24.5 \pm 7.4	31.4 \pm 8.9

(■) Not available.

average surface density of fibrocytes:

$p < 0.01$ at 1 week (Ti > 316L)
 $p < 0.01$ at 2 weeks (Ti > 316L)
 $p = 0.06$ at 26 weeks (Ti < 316L)
 $p < 0.01$ at 12 weeks + 26 weeks (Ti < 316L)

median surface density of fibrocytes:

$p < 0.01$ at 1 week (Ti > 316L)
 $p < 0.03$ at 2 weeks (Ti > 316L)
 There was a significant difference in the fibrocyte behaviour between stainless steel and pure titanium.

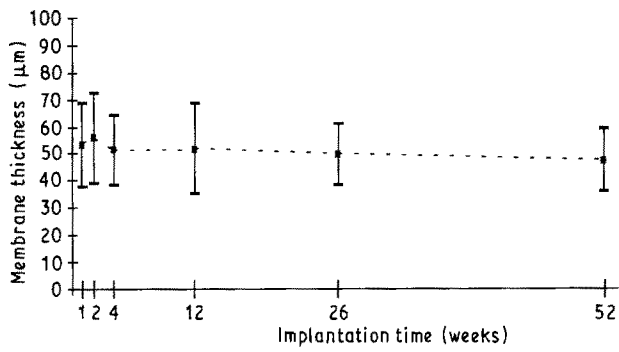


Figure 5 Time evolution of the encapsulating membrane thickness for all merged materials. The dotted line joins the means for each time of observation.

While the membrane surrounding CP Ti implants demonstrated a significant decrease in fibrocyte densities with time, the 316L membrane remained unchanged and even increased slightly over the long term. The linear correlation between implantation time and fibrocyte density was highly significant ($p < 0.01$ and $r = 0.75$) for CP Ti, but not for 316L ($r = 0.1$). However, there was no significant difference on the inflammatory cells' parameters; these cells were no longer observed for each material after 2 weeks.

3.3. CP Ti–Ti5Al2.5Fe comparison

Significant differences appeared for the following parameters:

linear density of fibrocytes:

$p < 0.02$ at 52 weeks (Ti < TiFe)

average surface density of fibrocytes:

$p < 0.03$ at 12 weeks (Ti < TiFe)

$p < 0.02$ at 52 weeks (Ti < TiFe)

In the long term, there were significantly more fibrocytes in the encapsulating membrane surrounding Ti5Al2.5Fe implants than those made of CP Ti. Moreover, the onset of the fibrocyte density decrease began earlier around CP Ti implants.

As for the previous comparison, there was no statistical significant difference noted for the parameters of the inflammatory cells.

3.4. CP Ti–Ti(TiO₂) comparison (Fig. 7)

The statistical analysis exhibited the following data:

linear density of fibrocytes:

$p < 0.01$ at 1 week (Ti(TiO₂) < Ti)

$p < 0.01$ at 1 week + 2 weeks (Ti(TiO₂) < Ti)

$p < 0.01$ at 52 weeks (Ti(TiO₂) > Ti)

$p = 0.06$ at 26 weeks + 52 weeks (Ti(TiO₂) > Ti)

average surface density of fibrocytes:

$p < 0.02$ at 4 weeks (Ti(TiO₂) < Ti)

$p < 0.01$ at 1 week + 2 weeks + 4 weeks (Ti(TiO₂) < Ti)

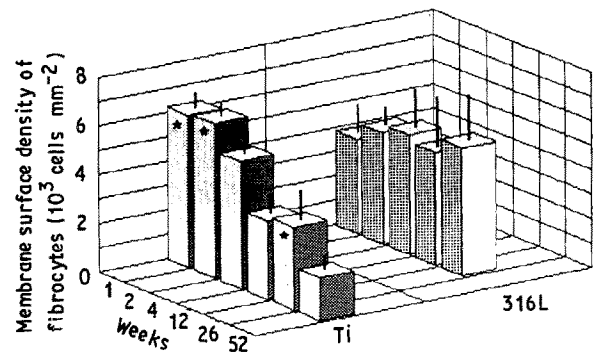


Figure 6 Membrane surface density for fibrocytes: comparison between CP Ti and 316L, means and standard deviations. (*) Significant differences, at $p < 0.05$, existing between the two materials, at 1, 2, and 26 weeks.

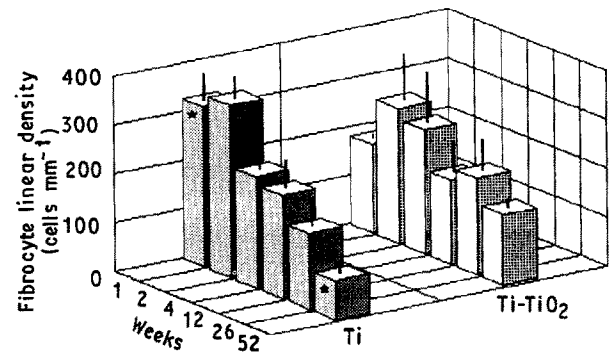


Figure 7 Time evolution of fibrocyte linear density within the encapsulating membrane: comparison between CP Ti and TiO₂-coated Ti (same remarks as Fig. 6).

median surface density of fibrocytes:

$p < 0.04$ at 4 week (Ti(TiO₂) < Ti)

polymorphonuclear cells linear density:

$p < 0.05$ at 1 week + 2 weeks (Ti(TiO₂) < Ti)

TiO₂-coated Ti induced some differences in the tissue response. There were significantly more fibrocytes as well as polymorphonuclear cells around the CP Ti implants in the early period post-implantation. However, this trend appeared to reverse after 1 year. The cell densities around CP Ti implants significantly decreased after 4 weeks, whereas such a decrease was not observed in the membranes surrounding TiO₂-coated Ti implants.

3.5. Ti6Al4V–Ti6Al4V (TiO₂) comparison

TiO₂-coated Ti6Al4V did not induce differences in the tissue response. Thus, statistically there was no difference although the theoretical parameters indicated that fibrocytes were closer to the interface with TiO₂-coated implant.

3.6. Ti6Al4V–Ti6Al4V (TiN) comparison

No difference in the twenty computed parameters, at any time of implantation, was found.

4. Discussion

Although the implant materials investigated in the current study are mainly aimed toward implantation in bone, the evaluation was carried out in muscle in accordance with the guidelines for biomaterials testing suggested by ISO. Soft tissues are more sensitive to differences in implanted materials than bone. Furthermore, orthopaedic devices are rarely exclusively in contact with bone tissue.

The cellular distribution in the encapsulated membrane exhibited several histomorphometric features which were identical for all the materials. Beyond 4 weeks, neither inflammatory nor giant cells were found in significant numbers. These data confirm the tissue tolerance of these materials which have, except for Ti5Al2.5Fe, been used in the clinical setting. For all the materials, the membrane thickness was not a time-dependent parameter. Other investigators [4] have attempted to use this as a criterion for biocompatibility; however, for the materials currently investigated, no statistically significant difference in the membrane thickness was noted when comparing all materials over our range of post-implantation periods. It appears that membrane thickness is insufficiently sensitive to be applied in the comparison of the close tissue reaction surrounding well-tolerated implant materials. It cannot be considered as representative of the overall tissue response. However, all the materials induced a close tissue reaction which was quantitatively analysed by histomorphometry. The notable differences in cellular response are:

- (i) in comparison to CP Ti, 316L induced the following fibrocyte response within the encapsulating membrane: in the short term, it induced a low amount of fibrocytes which did not decrease later on, contrary to titanium-based alloys;
- (ii) a similar trend was found for Ti5Al2.5Fe, although, for this material, the decrease in fibrocytes amount was slower than for CP Ti;
- (iii) in the short term, TiO₂-coated Ti induced a lower tissue reaction than CP Ti.

The similarities as well as the differences in the close tissue reaction could be attributed to several factors: surface energetics and chemistry, corrosion products, and surface roughness. The surface roughness of the implants investigated here were uniform. Roughness indexes given by the manufacturer were similar and the scanning electron micrographs (Fig. 1) did not show differences. Nevertheless, scarce defects could explain some data scatter which disturbed the statistical analysis. Considering the size of the implants, it appeared difficult to overcome this problem completely.

There are many reports of the surface chemistry and electrochemical properties of the materials used in this study in the literature [1, 15]. Pure titanium is naturally coated with an oxide layer (pure TiO₂ [16]) 5 nm thick which forms spontaneously over the metal surface exposed to the atmosphere. This passivated layer has a very high polarization resistance. Because it is not electron conductive, it limits the corrosion of the metal surface. Impurities (mainly Cl and F) are found

at, or near to the metal-oxide interface but are as stable as TiO₂. These foreign elements appear during the surface preparation process. In the current experiment, the TiO₂ layer deposited by electrolytical anodization on CP Ti and Ti6Al4V implants was 0.2 μm thick. This procedure leads to the formation of a clear limit between the metal substratum and the oxide layer with an increase in content of impurities (Cl, F and P), and pure metal disappearing from the surface [17]. In aqueous solution, as well as under physiological conditions, the titanium oxide layer transforms into Ti(OH)₄ which is uncharged, stable and at saturation in normal tissues [2]. Consequently, titanium *in vivo* releases only a small quantity of soluble products. In a biological situation, due to the amphoteric properties of Ti(OH)₄, amino acids which are also amphoteric can have a strong reversible bond to the material's surface [18]. The electrochemical behaviour of titanium may explain the excellent tolerance of this material and the histomorphometric data obtained in this study.

For the titanium alloys investigated here, Ti6Al4V and CP Ti induced identical reactions, whereas Ti5Al2.5Fe induced a small, yet significantly higher fibrogenesis than CP Ti in the long term. Although intrinsic vanadium toxicity is well known, vanadium in Ti6Al4V has not been demonstrated to be responsible for implant toxicity. This can be explained by the high polarization resistance of the Ti6Al4V oxide layer which is similar to that observed with CP Ti in the physiological situation [19]. Accordingly, the amount of vanadium ion release, in the absence of implant failure or fretting, is nearly negligible. The results presented by Gold *et al.* [20], supported this hypothesis by showing that vanadium was not detectable in the oxide layer before implantation or in the organic layer after implantation. Vanadium anions have a high solubility and would be dissolved in the first electrolytical bath during material preparation. Simpson [19] has shown that Ti5Al2.5Fe oxide layer has isolating properties lower than CP Ti in saline solution. Moreover, Zitter and Plenk [21] have discussed the possibility that a flow of electrons in the oxide may disturb the normal ion movement in the surrounding tissue by a redox reaction and therefore modify the tissue response. Although iron corrosion products (principally Fe(OH)₃) are uncharged, inert, and sparse, Zitter and Plenk's hypothesis could support the current results.

The 316L stainless steel behaviour could be explained by the same hypothesis as that applied for Ti5Al2.5Fe. The polarization resistance of stainless steel is lower than CP Ti, so the redox reaction could disturb the fibrocyte kinetics.

5. Conclusion

When comparing CP Ti, TiO₂-coated Ti, Ti6Al4V, TiO₂-coated Ti6Al4V, TiN-coated Ti6Al4V, Ti5Al2.5Fe, and 316L stainless steel, it appeared that all materials induced a close tissue reaction. There was no statistical difference between the tested materials regarding the time-evolution of the inflammatory cells

which disappeared after 4 weeks' implantation. The membrane thickness was identical for all tested materials and appeared not to be time-dependent. However, quantitative histomorphometry allowed the differences in fibrocyte kinetics between the materials implanted to be distinguished. Thus, while pure titanium demonstrated a significant decrease in fibrocyte densities with time, densities for 316L, and to a lesser extent Ti5Al2.5Fe, remained unchanged. In the short term, surface treatments modified the tissue response only for anodized CP Ti for which the tissue reaction is lower than CP Ti. Considering biocompatibility parameters, when the implants are not damaged, surface treatments or vanadium substitution with iron do not decrease the tissue response when compared to Ti6Al4V.

Acknowledgements

The implants were supplied by the Ceraver-Ostéal company (Mr D. Blanquaert). The authors thank Mrs C. Schiltz for technical assistance. This study was partly supported by Ceraver-Ostéal and CNRS.

References

1. S. G. STEINEMANN and P. A. MAUSLI, "Titanium alloys for surgical implants - biocompatibility from physicochemical principles", in Proceedings, Part I of the 6th World Conference on Titanium, Cannes, France, 6-9 June 1988.
2. S. G. STEINEMANN, "Corrosion of implant alloys", in Proceedings of the 3rd Biomaterials Symposium: Technical Principles, Design and Safety of Joint Implants, Göttingen, 22-25 June 1987.
3. D. L. COLEMAN, R. N. KING and J. D. ANDRADE. *J. Biomed. Mater. Res. Symp.* **5** (part I) (1974) 65.
4. P. G. LAING, A. G. FERGUSON and E. S. HODGE. *J. Biomed. Mater. Res.* **1** (1967) 135.
5. H. PLENK, "Techniques of Biocompatibility Testing", Vol. I, edited by D. F. Williams (CRC Press, Boca Raton, FL, 1986) p. 35.
6. R. H. RIGDON, *J. Biomed. Mater. Res.* **7** (1973) 79.
7. D. F. WILLIAMS (ed.), "Techniques of biocompatibility testing", Vol. I (CRC Press, Boca Raton, FL, 1986) p. 83.
8. S. C. WOODWARD and T. N. SALTHOUSE, in "Handbook of Biomaterials Evaluation - Scientific, Technical, and Clinical Testing of Implant Materials", edited by A. F. von Recum (Macmillan, New-York, 1986) p. 364.
9. J. E. TURNER, W. H. LAWRENCE and J. AUTIAN, *J. Biomed. Mater. Res.* **7** (1973) 39.
10. B. A. RAHN, V. GERET, C. CAPUL, M. LARDI and B. SOLSTRHURNAMM. in "Clinical Applications of Biomaterials", edited by A. J. C. Lee, T. Albrektsson and P. I. Branemark (Wiley, New York, 1982) p. 263.
11. P. CHRISTEL and A. MEUNIER, *J. Biomed. Mater. Res.* **23** (1989) 1169.
12. P. CHRISTEL, A. MEUNIER and M. THERIN, *J. Appl. Biomater.* **1** (1990) 205.
13. K. V. BURY, "Statistical Models in Applied Sciences" (Wiley, New York, 1975).
14. W. WEIBULL, *Trans. ASME* **73** (1951).
15. L. L. HENCH and E. C. ETHRIDGE. "Biomaterials: An Interfacial Approach" (Academic Press, New York and London, 1982) p. 8.
16. P. A. MAUSLI, J. P. SIMPSON, G. BURRI and S. G. STEINEMANN, in "Implant Materials in Biofunction" edited by C. Putter, G. L. de Lange, K. de Groot and A. J. C. Lee, *Advances in Biomaterials*, Vol. 8 (Elsevier, Amsterdam, 1988) p. 305.
17. P. A. MAUSLI, P. R. BLOCH, V. GERET and S. G. STEINEMANN, in "Biological and Biomechanical Performance of Biomaterials", edited by P. Christel, A. Meunier and A. J. C. Lee (Elsevier, Amsterdam, 1986) p. 57.
18. J. M. GOLD, M. SCHMIDT and S. G. STEINEMANN, *Helv. Phys. Acta* **62** (1989) 246.
19. J. P. SIMPSON, in "Biological and Biomechanical Performance of Biomaterials", edited by P. Christel, A. Meunier and A. J. C. Lee (Elsevier, Amsterdam, 1986) p. 63.
20. J. M. GOLD, M. SCHMIDT and S. G. STEINEMANN, "Clinical implant materials", edited by G. Heimke, U. Soltesz and A. J. C. Lee, (Elsevier, Amsterdam, 1990) p. 69.
21. H. ZITTER and H. PLENK, *J. Biomed. Mater. Res.* **21** (1987) p. 881.

Received 11 April
and accepted 14 August 1990